Molecular Dynamics Simulations of Ion Solvation by Flexible-Boundary QM/MM: On-the-fly Partial Charge Transfer between QM and MM Subsystems

Soroosh Pezeshki and Hai Lin*

The flexible-boundary (FB) quantum mechanical/molecular mechanical (QM/MM) scheme accounts for partial charge transfer between the QM and MM subsystems. Previous calculations have demonstrated excellent performance of FB-QM/MM in geometry optimizations. This article reports an implementation to extend FB-QM/MM to molecular dynamics simulations. To prevent atoms from getting unreasonably close, which can lead to polarization catastrophe, empirical correcting functions are introduced to provide additive penalty energies for the involved atom pairs and to improve the descriptions of the repulsive exchange forces in FB-QM/MM calculations. Test calculations are carried out for chloride, lithium, sodium, and ammonium ions solvated in water. Comparisons with conventional QM/MM calculations suggest that the FB treatment provides reasonably good results for the charge distributions of the atoms in the QM subsystems and for the solvation shell structural properties, albeit smaller QM subsystems have been used in the FB-QM/MM dynamics simulations.

DOI: 10.1002/jcc.23685

Introduction

Combined quantum mechanical and molecular mechanical (QM/MM)[1–16] calculations have gained popularity in the past decade. A QM/MM model divides an entire system into a primary system (PS) described at the QM level and a usually much larger secondary system (SS) at the MM level. The PS is of our primary interest, and it is under the influence of the environmental SS. The combination of the high-accurate QM treatment for the PS and computationally efficient MM for the SS makes QM/MM a powerful tool in the studies of many chemical, physical, and biological processes.

One of the limitations in conventional QM/MM calculations is that partial charge transfer between the PS and SS is prohibited. Such partial charge "leakage" from one subsystem to the other is, however, certainly possible in many situations, for example, through hydrogen-bonds that connect the PS and SS.[17] To gain a more realistic picture, it is highly desirable to go beyond the limit by allowing partial charge transfer between the two subsystems.

Recently, Zhang and Lin[17,18] developed the Flexible-Boundary (FB) QM/MM method for this purpose. In this method, the PS can exchange partial charges, according to the principle of electronic chemical potential equalization and charge conservation, with the SS atoms that are near the QM/MM boundary. Those SS atoms are often referred to as MM boundary atoms. Due to the screening effect, the SS atoms that are further away from the boundary are deemed insignificantly affected by the partial charge transfer between the PS and SS, and they are thus not included in the FB treatments. The principle of electronic chemical potential equalization (also known as the principle of electronegativity equalization) has been applied to model the polarization and charge transfer in classical force fields.[19–34] The works by Zhang and Lin[17,18] have extended it to treat charge transfer between the quantum and classical subsystems. Test calculations[17,18] of the FB-QM/MM method on a series of model systems showed that the FB treatments can provide reasonably good agreements in the atomic charges for the PS when compared with the full-QM calculations of the entire system. The FB treatments also led to substantially improved bond distances in geometry optimizations for the covalent bonds that connect the PS and SS in comparisons with the calculations without the FB treatments.

In this work, we report our implementation to extend the FB-QM/MM scheme to molecular dynamics (MD) simulations. In MD simulations, a molecule may be substantially distorted from the equilibrium geometry, and atoms may occasionally come in close contacts. How robust are the FB-QM/MM schemes in handling those situations far from ideal? This is the topic that we want to explore in this contribution, and we will test the FB-QM/MM MD simulations on several models for ions solvated in water.

S. Pezeshki H. Lin
Chemistry Department, CB 194, University of Colorado Denver, PO Box 173364, Denver, Colorado, 80217
E-mail: hai.lin@ucdenver.edu
Author Contributions: H.L. formularized the algorithm. S.P. did the programming and calculations. S.P. and H.L. wrote the article together.
Disclosure: The authors declare no competing financial interest.
Contract grant sponsor: National Science Foundation; Contract grant number: CHE-0952337; Contract grant sponsor: Extreme Science and Engineering Discovery Environment; Contract grant number: CHE-140070

Methods

FB treatments

The FB-QM/MM method has been described previously.[17,18] Here, we only give a brief outline. Basically, two questions need to be answered. The first question is how to treat a QM subsystem with fractional electrons, because partial charges are transferred between the PS and SS. Several schemes have been proposed, including Dewar's half-electron method[35,36] and its extension by Gogonea and Merz,[37,38] the treatment of fractional particle number in density functional theory by Perdew et al.[39] and the further development by Yang and coworkers,[40–47] the molecule-in-molecule method by Mayhall and Raghavachari,[48] and the density functional partition theory with fractional occupations by Wasserman and coworkers.[49,50] Our approach[17,18] is similar to the one used by Tavernelli et al.,[51] where the fractional electrons are realized from the thermodynamics instead of the electronic-structure point of view. We consider the PS as a statistical mixture of reduced and oxidized states of different charges and spins but the same geometry. Embedded-QM calculations will be carried out for both oxidization states with integer charges. Certain properties such as the energy E(PS) and atomic charges q_i(PS) of the PS are then computed as ensemble averages:

$$E(\mathrm{PS}) = x_+ E(\mathrm{X}^+) + xE(\mathrm{X}) \quad (1)$$

$$q_i(\mathrm{PS}) = x_+ q_i(\mathrm{X}^+) + xq_i(\mathrm{X}) \quad (2)$$

Here, x_+ is the molar fraction of the oxidized state X^+, and $x = (1 - x_+)$ is the molar fraction for the reduced state X. This treatment is conceptually simple and straightforward to implement, making it easy to use any QM level of theory and most existing QM program packages.

The second question is how much charge (q) should be transferred between the PS and SS. Our answer is based on the principle of electron chemical potential equalization. (Note that electronegativity is the negative of the electronic chemical potential, μ.) For the SS at the MM level, the electron chemical potential μ(SS) is obtained by a classical electronegativity equalization model. We have used the QEq model by Rappé and Goddard[22] (with our extension to include the electrostatic potential due to the PS), which also takes care of the redistributions of the transferred charges in the SS (as done in the polarized-boundary QM/MM scheme).[52] For the PS at the QM level, the electron chemical potential depends on the energies of the reduced state E(X) and of the oxidized state $E(X^+)$ as well as an entropic contribution

$$\mu(\mathrm{e}^-) = E(\mathrm{X}) - E(\mathrm{X}^+) + k_B T_e \ln(x/x_+) \quad (3)$$

Here, k_B is the Boltzmann constant and T_e is the electronic temperature. T_e is a parameter that signifies the tendency of the PS exchanging electrons with the SS (not to be confused with the temperature for nuclear motions). When charge transfer occurs between the two subsystems, the molar fractions of the reduced and oxidized states of the PS vary, and so do the electronic chemical potentials of both the PS and SS. The charge transfer ceases when equilibrium is reached for chemical potentials between the PS and SS. We have used an iterative protocol to determine q variationally.[17]

An issue is how to calibrate the electronic chemical potentials of the PS and SS, which are computed at two different levels of theory. This can be achieved by requiring that the electronic chemical potentials of the PS and of the SS have the same value[17] and the same slope $(\partial\mu/\partial q)$[18] at $x^+ = x = 0.5$, where the entropic term in eq. (3) vanishes. The details have been already provided in the literature[17,18] and will not be repeated here. We just want to point out that the requirement of the same slope provides an automate way[18] to determine the parameter T_e. It should also be noted that the FB treatments optimize only the parameters for the one-electron terms that enter the effective-QM Hamiltonian for the embedded-QM subsystem and do not alter the point charges in the involved MM calculations. Therefore, the FB treatments do not lead to inconsistency in the MM calculations.

Extension to MD simulations

A system treated by the FB scheme in the MD simulations can be regarded as moving smoothly on a potential energy surface of mixed reduced and oxidized state, and the energy would be conserved. Therefore, one may think that the application of the FB treatments to MD simulations is trivial and straightforward. However, in MD simulations, a molecule may be substantially distorted from the equilibrium geometry, and atoms may occasionally come in close contacts. Can our FB scheme handle those challenging situations?

Those situations are challenging because the QEq model (and other classical models based on the principle of electronegativity equalization) are usually parameterized against reference data for molecules at or near equilibrium geometries. Those models might not behave as well for systems with geometries far from equilibrium. Without any measures to modify the interactions between the atoms in close distances, polarization catastrophe can occur, which leads to numerical instability and even the crash of the simulations. That has been observed in our test calculations.

The prescription that we take in this work to overcome the above difficulty is to introduce an empirical correcting function that provides an additive "penalty" energy term when the involved pair of atoms are in close distances. The penalty energy discourages the atoms from getting unreasonably close to the point where the polarization catastrophe may occur. The correcting procedure is equivalent to amend the repulsive exchange forces due to the Pauli Exclusion Principle, which are typically computed as the repulsive component of the van der Waals (vdW) interactions in an MM force field.

The vdW interactions in a "standard" MM force field are designed to work with the other MM force field parameters. They are not parameterized for FB-QM/MM calculations. In principle, one should reoptimize the vdW parameters in the FB-QM/MM calculations so that the interatomic interactions

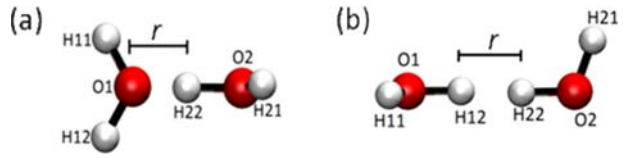

Figure 1. Initial geometries for energy surface scans. a) For OW(QM)-HW(FB) and OW(FB)-HW(QM) interactions. $r = 0.55$ Å, plane H21-O2-H21 bisects angle H11-O1-H12, and dihedral H21-O2-H22-O1 = 4.5°. b) For HW(QM)-HW(FB) interactions. $r = 0.5$ Å, dihedral H21-O2-H22-H12 = 25°. In all energy scans, the step sizes are $dr = 0.1$ Å. [Color figure can be viewed in the online issue, which is available at wileyonlinelibrary.com.]

including the repulsive exchange forces can be better described. However, this is difficult to achieve, because the FB-QM/MM energy depends in a complex way on the MM atomic charges in the SS, the electric field generated by the PS, and the distances and relative orientations between the involved molecules. The correcting function introduced in this work provides an alternative way to empirically improve the descriptions of the repulsive exchange forces while leaving the existing vdW parameters unmodified. Although the solution is probably not optimal, it is conceptually straightforward and relatively easy to implement.

We note that such a correcting procedure was not used in our previous FB-QM/MM calculations.[17,18] That is because the repulsive exchange forces are significant only in short distances. Consequently, the amendment was not needed in our previous test calculations based on geometry optimizations, where the atoms were not in very close distances. For MD simulations in this study, however, the update of the repulsive exchange forces would be important.

Correcting-function parameterization

The correcting function takes the following form:

$$f(r) = A_0 + A_1 r^{-1} + A_2 r^{-2} + A_3 r^{-3} + A_4 r^{-4} \quad (4)$$

where $0 < r < r_{max}$ is the distance between the involved pair of atoms and the coefficients A_n ($n = 0, 1, \ldots 4$) depend on their atom types. For $r > r_{max}$, the correction is set to 0. Because we will study the solvation of ions in water in this article, we consider the pairs among the water oxygen (OW) and water hydrogen (HW) atoms, in particular, the following five atom-type pairs: OW(QM)-HW(FB), OW(FB)-HW(QM), HW(QM)-HW(FB), HW(FB)-HW(FB), and HW(FB)-HW(MM), where QM denotes a QM atom, FB an MM boundary atom whose atomic charge will vary in FB calculations, and MM an "ordinary" MM atom whose atomic charge will be fixed all the time. To reduce the number of fitted parameters, we have required that OW(QM)-HW(FB) and OW(FB)-HW(QM) have the same correcting functions and that HW(FB)-HW(FB) and HW(FB)-HW(MM) have the same correcting functions. Furthermore, as demonstrated in Figure S1 in the Supporting Information, the OW(QM)-OW(FB) interactions are very repulsive, and consequently, no correcting function was needed.

The requirements of the correcting function are that it should reshape the FB-QM/MM energy curve such that the corrected curve bears resemblance to the full-QM energy curve as much as possible when the pair of atoms are in medium to short distances of r (ca. 0.7 to 1.5 Å) and that it should be strongly repulsive for even shorter distances. The coefficients A_n are determined in a fitting procedure. The procedure is exemplified here by the OW(QM)-HW(FB) interactions. Two water molecules, each at its QM-optimized geometry, are placed together, as shown in Figure 1a. Energy surface scans are performed, where the distance between the oxygen O1 and hydrogen H22 atoms are increased from 0.55 to 2.95 Å with a step size of 0.1 Å. For each geometry in the surface scan, two sets of single-point calculations are carried out: full-QM and FB-QM/MM, respectively. The full-QM calculations, where both water molecules are treated at the QM level of theory, provides the reference interaction potentials for the parameterizations. In the FB-QM/MM calculations, the first water molecule is treated by QM, and the second by the FB method. The coefficients A_n are adjusted by minimizing the error function

$$\mathrm{Err} = \Sigma_i [f(r_i) - \Delta E(r_i)]^2 \quad (5)$$

where r_i is the distance between the involved pair of atoms, ΔE the difference between the full-QM and FB-QM/MM energies

$$\Delta E(r_i) = E_{\text{full-QM}}(r_i) - E_{FB\text{-QM/MM}}(r_i) \quad (6)$$

and the sum is over all data points in the surface scan. A similar fitting process is applied for the HW(QM)-HW(FB) interactions, where the initial geometry is illustrated in Figure 1b. The distance between the two hydrogen atoms H12 and H22 are scanned from 0.5 to 3.0 Å.

For the HW(FB)-HW(FB) interactions, we have used a three-water model complex for technical convenience. The first and second water molecules take the same initial geometry as in Figure 1b, while the third water molecule is placed about 20 Å away from the first and second molecules (along a line in the H11-O1-H12 plane and perpendicular to line H12-H22). The third water molecule is so far away from the other two molecules that it has minimal effects on them. In the FB-QM/MM calculations, the third water molecule is treated by QM, whereas the first and second are treated by the FB methods. Energy scans are performed with the distance between H12 and H22 from 0.5 to 3.0 Å.

The finalized A_n are tabulated in Table 1, along with the values for r_{max}, which has been introduced to keep the corrections in short ranges only. The values of r_{max} are selected empirically, based on exploratory short-time simulations. The hydrogen–hydrogen pairs have larger r_{max} values while the oxygen–hydrogen pairs have a smaller one, because of the different (repulsive versus attractive) electrostatic forces between the atoms pairs. The discontinuity at $r = r_{max}$ is eliminated by modifying the optimized A_0, that is, by vertically shifting the corrected curve, such that the corrected curve superimposes with the curve without correction at $r = r_{max}$. Figure 2 demonstrates in the short to medium distances of r, the reference

Table 1. Coefficients A_n (n = 0, 1, . . ., 4) for the correcting function.[a]

	OW(QM)-HW(FB) and OW(FB)-HW(QM)	HW(QM)-HW(FB)	HW(FB)-HW(FB) and HW(FB)-HW(MM)
A_0 (E_h)	-2.49735×10^2	1.3826×10^{-1}	1.17837×10^{-2}
A_1 (E_h/Å)	4.11942×10^2	-6.82798×10^{-1}	-6.42912×10^{-2}
A_2 (E_h/Å^2)	-2.38165×10^2	1.22407	9.01361×10^{-2}
A_3 (E_h/Å^3)	5.75062×10^1	-9.81811×10^{-1}	-6.70845×10^{-3}
A_4 (E_h/Å^4)	−3.93202	0.33205	2.32565×10^{-3}
r_{max} (Å)	0.75	1.80	2.70

[a] Defined by eq. (4) for $0<r<r_{max}$. OW denotes water oxygen, and HW water hydrogen. QM denotes QM atoms, FB boundary MM atoms, and MM ordinary MM atoms.

full-QM curve, the FB-QM/MM curves without and with corrections, as well as the amount of charge transfer between the PS and SS.

The transferability of the coefficients A_n are then tested in additional energy surface scans with additional orientations of the two water molecules (see Fig. S2 in the Supporting Information), where correcting functions are applied to all involved pairs. Overall, the applications of the correcting functions have led to reasonably good agreements in the medium to short range of r and strongly repulsive at short r distances. (Because the correction does not apply in the long r distances, the system is not affected there.)

Simulations of ion solvation

The FB-QM/MM method is applied to MD simulations of four different types of ions in water using droplet models. The selection include one monatomic anion (Cl^-), two monatomic cations (Li^+ and Na^+), and one polyatomic cation (NH_4^+). The solvation structures and dynamics of those ions in water have been extensively investigated by computations. For example, the Car–Parrinello dynamics[53] has been applied to examine the hydration of Cl^-,[54–56] Li^+,[57,58] and Na^+[59] ions. Other examples are the QM/MM dynamics simulations of the Cl^-,[60–65] Li^+,[62,66,67] Na^+,[60,62,65,68–70] and NH_4^+.[71,72] Those theoretical investigations have contributed significantly to our understanding of those hydrated ions. However, a detailed review of those results is beyond the scope of this study, and we refer the readers to recent review articles[73–75] for further discussion. Because we are concentrated on the test of the applicability of the FB-QM/MM in MD simulations, we are not pursuing the agreements between the FB-QM/MM calculations and other computational or experimental data.

As illustrated in Figure 3, each model consists of an ion (denoted as C) located at the center of the droplet and surrounded by 1482 SPC water molecules (density = 1.00 g/mL). The water droplet, which is pre-equilibrated at the MM level, has a radius of r_{ME} = 22 Å. In the FB-QM/MM simulations, the water molecules are divided into four layers according to their distances r_c to the ion: the innermost QM layer ($r_c \le r_{PS1}$) described at the QM level, the second FB layer ($r_{PS1} < r_c \le r_{PS2}$) for the MM boundary atoms whose atomic charges will vary in the FB treatment, the third electrostatic-embedding layer ($r_{PS2} < r_c \le r_{EE}$) where the fixed atomic charges enter the effective QM Hamiltonian, and the outermost mechanical-embedding (ME) layer ($r_{EE} < r_c$) whose atoms interacts with the atoms in the other layers via Coulomb's Law using the MM point charges at all water molecules and the formal charges at the ions (for polyatomic ion NH_4^+, q(N) = −0.40 e, and q(H) = 0.35 e). The water oxygen atoms in the ME layer are restrained to its original positions by harmonic potentials with force constants of 20 kcal/mol/Å^2. The ME layer acts as an effective barrier that prevents the water molecules in the other three layers from escaping into the vacuum. The value of 4 Å for r_{PS1} is approximately the radius of the first solvation shell of the central ion, that is, the ion and its first solvation shell are

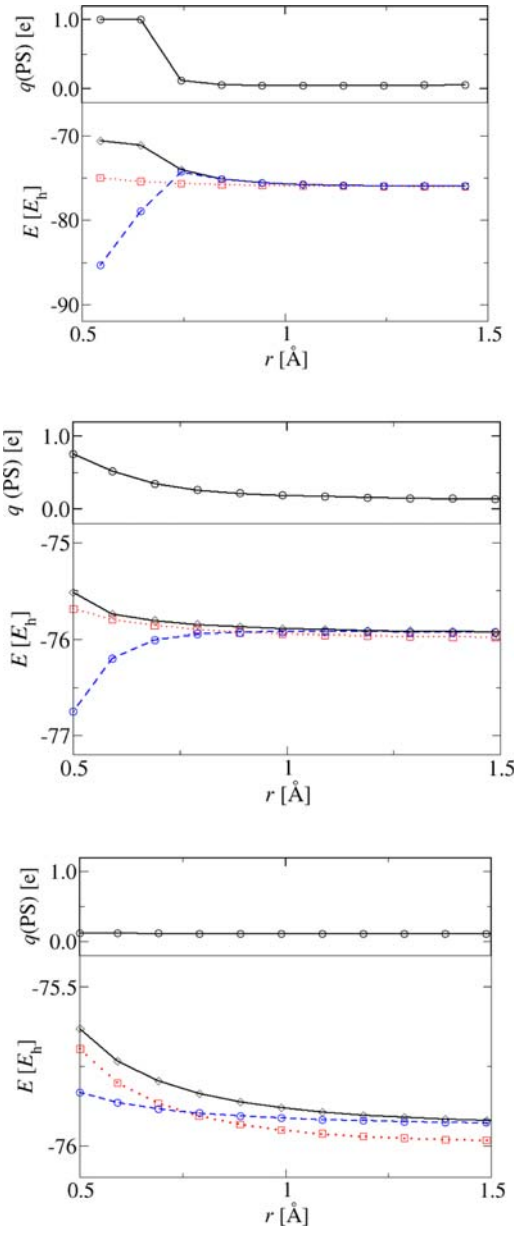

Figure 2. The reference full-QM energy (dotted), the FB-QM/MM energies without corrections (dashed), and with corrections (solid) for the correcting function parameterization. The charges at the PS are also shown. Upper panel: OW(QM)-HW(FB), middle panel: HW(QM)-HW(FB), and lower panel: HW(FB)-HW(FB). [Color figure can be viewed in the online issue, which is available at wileyonlinelibrary.com.]

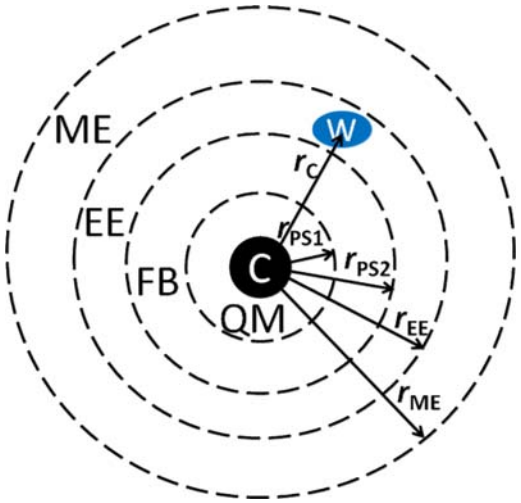

Figure 3. Schematics of the four layers of the droplet model in the FB-QM/MM simulations of ion solvation. The central ion is denoted C. According to its distance (r_C) from C, a water molecule (W) will be treated by QM, by the FB schemes, by the electrostatic-embedding scheme, or by the mechanical-embedding (ME) scheme. r_C is measured between the centers of mass of the ion and of the water. The water oxygen atoms in the outmost (ME) layer are restrained to its original positions by harmonic potentials with force constants of 20 kcal/mol/Å^2. [Color figure can be viewed in the online issue, which is available at wileyonlinelibrary.com.]

treated at the QM level. The values are 6 Å for r_{PS2} and 8 Å for r_{EE}, respectively.

The QM level of theory is set to the Hartee–Fock[76] level with the 6-31G[77–80] basis set for computational efficiency. One can certainly choose a higher level of QM theory, but for the purpose of testing the FB-QM/MM for MD simulations, the current selection suffices. Higher QM level of theory and larger basis set will be used in the future for achieving agreements with experimental results, which will be our next step of development. The OPLS force fields[81–84] are used together with the SPC water model[85] for the MM calculations. Simulations are performed using the QMMM 2.0.0.CO software package.[86] QMMM calls Tinker[87] for MM calculations and Gaussian03[88] for QM calculations. The electron temperature was determined by the automated method in the QMMM program as described earlier.[17] Each model system was minimized and then equilibrated for 1 ps in an NVT ensemble before productive MD runs are carried out for 4 ps. The time step length was set to 1 fs/step. The temperature was set to 300 K with a Berendsen thermostat.[89] The cutoffs for the vdW and electrostatic are 14 Å, with switching functions applied to taper both interactions beginning at 13 Å. To check the equilibration of the model system, we have plotted the velocity autocorrelation functions for the atoms in the QM and FB layers in the Figure S3 in the Supporting Information. The plots suggest that the equilibration time of 1 ps was sufficient for the used model systems. The trajectories are saved every step. For each ion, a number of independent trajectories are propagated in parallel from different starting configurations, providing trajectories combined of at least 30 ps in total for data analysis. A brief summary of the number of independent trajectories and total lengths of productive runs are given in Table S1 in the Supporting Information.

For comparisons, we have also performed conventional QM/MM simulations with a larger PS (denoted QM/MM-LPS) and pure-MM (denoted MM) simulations, both using the same model systems as in the FB-QM/MM simulations. The QM/MM-LPS results serve as the reference for the FB-QM/MM results to match, just like full-QM calculations as the reference for QM/MM calculations to compare. In the QM/MM-LPS simulations, the molecules in the FB layer are also treated at the QM level. (The conventional QM/MM calculations where the PS contains only the QM layer can be called QM/MM with smaller PS or QM/MM-SPS for short.) The other setups are the same as those in the FB-QM/MM simulations except that in the pure-MM simulations, owing to the lower computational costs, longer equilibration (10 ps each) and productive run (90 ps each) are performed, and the trajectories are saved every 100 steps.

Results and Discussion

Charge transfer between PS and SS

First, we look at the charges transfers between the PS and SS during the MD simulations, which will not be possible in QM/MM-SPS simulations. The total amounts of transferred charge are reflected by the total charge for all atoms in the QM layer as shown in Figure 4. Reasonable agreements can be seen

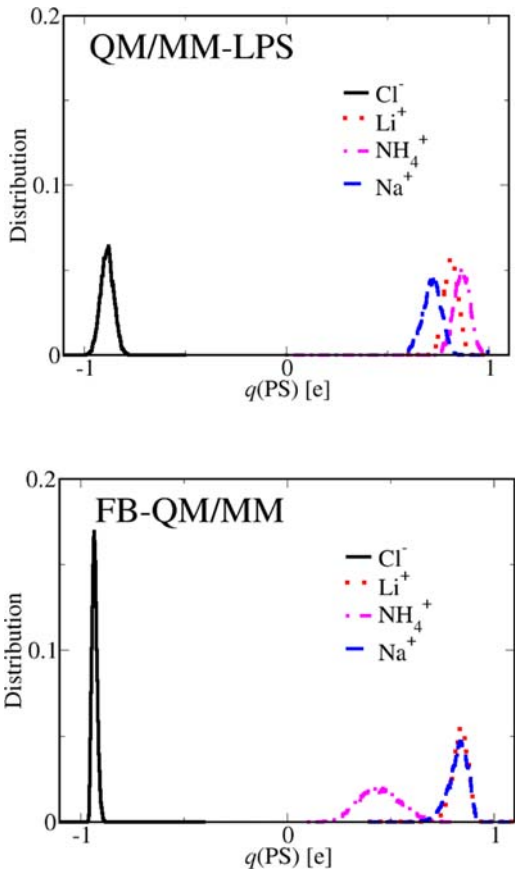

Figure 4. Distributions of the total charge in the MD simulations for the atoms in the QM layer. The QM/MM-LPS results are shown in the upper panel, while the FB-QM/MM data in the lower panel. [Color figure can be viewed in the online issue, which is available at wileyonlinelibrary.com.]

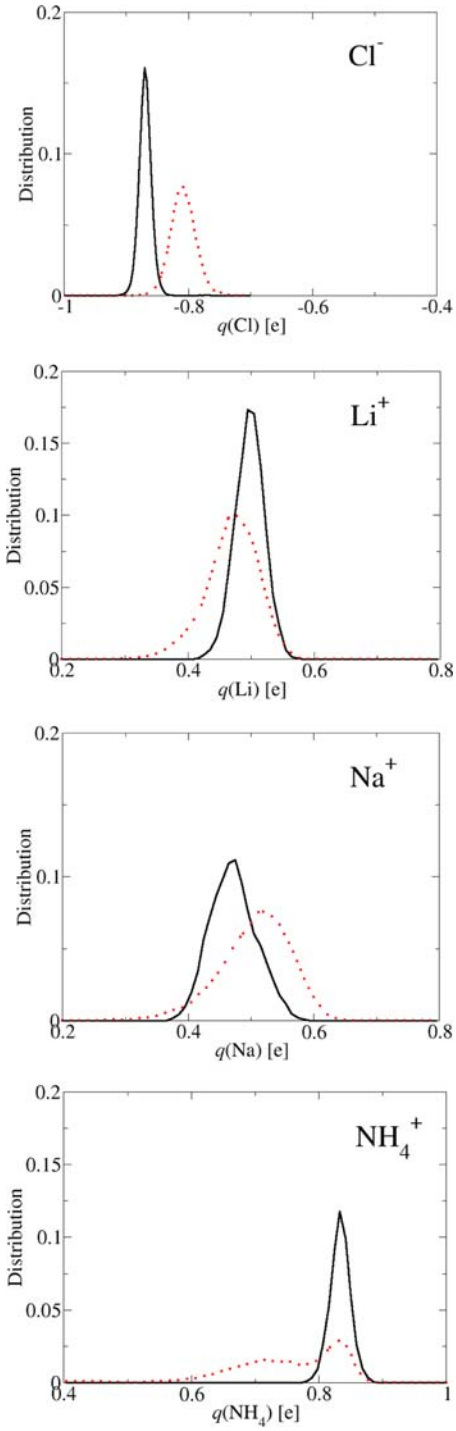

Figure 5. Distributions of charge of the ions by simulations using QM/MM-LPS (solid curves) and using FB-QM/MM (dotted curves). [Color figure can be viewed in the online issue, which is available at wileyonlinelibrary.com.]

between the QM/MM-LPS and the FB-QM/MM results. The best agreement is observed for the Li^+ model system, where both results match each other very well. The agreement for Cl^- is also quite good, although the FB-QM/MM results display a narrower distribution. For Na^+, FB-QM/MM underestimates the amount of charge transfer by about 0.1 e, shifting the distribution to the right in the plot. The largest discrepancy is found for NH_4^+, where FB-QM/MM overestimates the extent of charge transfer by about 0.3 e and also shows a wider distribution.

The amount of charge transfer between the PS and SS is determined by the electronic chemical potentials computed at the QM for the PS and by the classical QEq model for the SS. The accuracy depends on, to a large extent, the parameterizations of the QEq model. We expect that the agreements will improve if the QEq model is reparameterized specifically for the FB-QM/MM schemes. Such reparameterizations are beyond the scope of this work, which is to test the feasibly of the FB scheme in MD simulations. Therefore, we have not carried out the reparameterizations and will leave them to the next study.

Atomic charges of PS atoms/groups

Here, the Löwdin charges of the PS atoms and groups are compared. (It is well known that each charge model has its pros and cons, and one can choose other charge models for the present analysis, but the result will be qualitatively similar.) Figure 5 shows the charge distributions for the ions from the simulations. For each of the ions except NH_4^+, the FB-QM/MM simulations give a single peak in the charge distribution, whose location is within 0.1 e from the peak location by the QM/MM-LPS simulations. The FB-QM/MM results for NH_4^+ display one peak at the same location as in the QM/MM-LPS curve and one shoulder at about 0.7 e. Overall, the FB-QM/MM charge distributions are slightly broader than those by QM/MM-LPS calculations, with again the only exception NH_4^+, for which the shoulder at about 0.7 e has lead to quite substantial broadening.

In Figures 6 and 7, we plot the charge distributions for the oxygen and hydrogen of water, respectively, for the model systems. For the atoms in the QM layer, the FB-QM/MM calculations agree with QM/MM-LPS very well, with the difference usually being 0.02 e or less. The only exception is the OW atoms in the Cl^- model system, and their charge distributions are centered around -1.02 e in the FB-QM/MM calculations, which are larger by 0.05 e in magnitude than the charges in the QM/MM-LPS calculations. For the atoms in the FB layer, the charges obtained by FB-QM/MM are not the Löwdin charges; instead they are based on the classical QEq model: -0.71 to -0.74 e for OW and 0.35 to 0.37 e for HW. Not surprisingly, those charges differ significantly from the Löwdin charges shown for the QM/MM-LPS results.

Structural properties

Next, we examined the structural properties, in particular, the radial distribution functions (RDF) for the solvated ions. To check the capability of the droplet model in giving reasonably good RDF for the inner (QM and FB) layers, we have computed the RDF obtained at the MM level using the periodic boundary conditions (PBC). The PBC simulations were carried out in the NVT ensemble at the same temperature, using a cubic box of $36 \times 36 \times 36$ Å^3, with the same setups for vdW and electrostatic tapering, and yielded 540 ps productive trajectory. The PBC-based RDF are compared with the RDF obtained at the MM level using the droplet model, which is exemplified by the

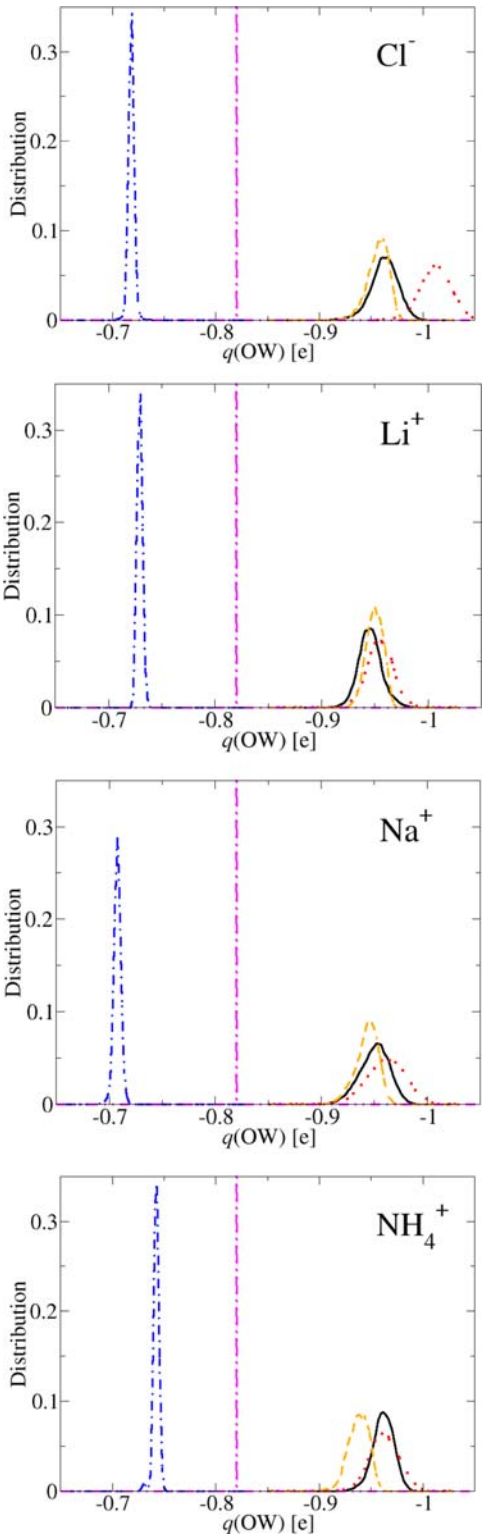

Figure 6. Distributions of atomic charges of the water oxygen (OW). For atoms in the QM layer, the QM/MM-LPS results are shown by the solid curves, and the FB-QM/MM results by the dotted curves. For atoms in the FB layer, the QM/MM-LPS data are given by dashed curves, and the FB-QM/MM results by dotted-dashed curves. The dotted-dashed straight lines indicate the fixed atomic charge in the SPC-water force field. [Color figure can be viewed in the online issue, which is available at wileyonlinelibrary.com.]

RDF for the Cl^--OW pair in Figure S4 in the Supporting Information. It can be seen that the agreement are excellent up to r(Cl-OW) = 8 Å, covering both the QM and FB layers,

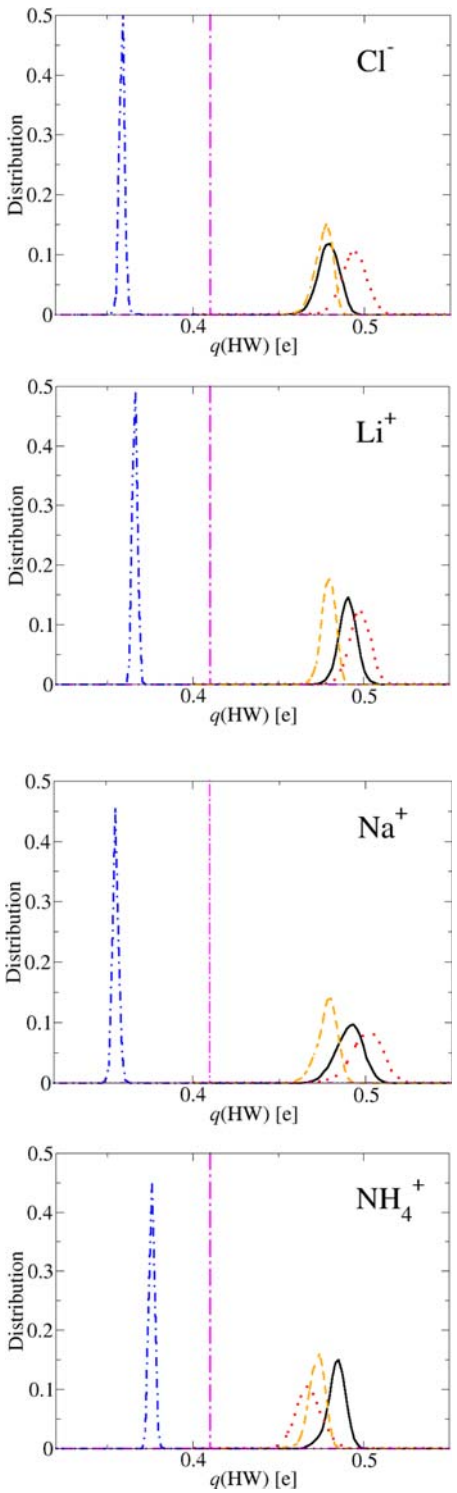

Figure 7. Distributions of atomic charges of the water hydrogen (HW). For atoms in the QM layer, the QM/MM-LPS results are shown by the solid curves, and the FB-QM/MM results by the dotted curves. For atoms in the FB layer, the QM/MM-LPS data are given by dashed curves, and the FB-QM/MM results by dotted-dashed curves. The dotted-dashed straight lines indicate the fixed atomic charge in the SPC-water force field. [Color figure can be viewed in the online issue, which is available at wileyonlinelibrary.com.]

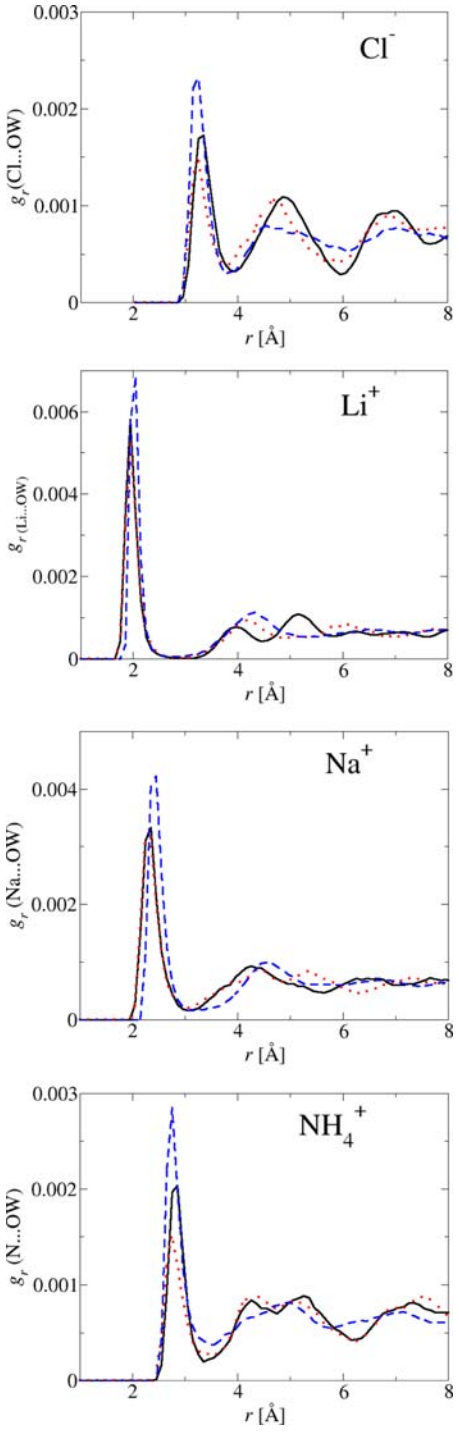

Figure 8. RDF for the X-OW pairs, where X = Cl, Li, Na, and N, respectively. The QM/MM-LPS results are shown by the solid curves, the FB-QM/MM results by the dotted curves, and the MM results by dashed curves.

indicating negligible effects due to the restraints imposed on the outmost ME-layer atoms.

The RDF for the X-OW pairs (X = Cl, Li, Na, and N) in the ion model systems are plotted in Figure 8. Overall, the FB-QM/MM results are rather similar to the QM/MM-LPS results, especially for $r<r_{PS1}$ = 4Å. Between 4 and 6 Å, which corresponding to the FB layer, the FB-QM/MM and QM/MM-LPS results are in good agreements for the Cl^- and NH_4^+ model systems, but deviate from each other when $r > 5$ Å for Li^+ and Na^+. Both the QM/MM-LPS and FB-QM/MM results differ from the MM simulations considerably.

Those structural differences are also echoed in the integrated coordination numbers shown in Figure 9. The FB-QM/MM and QM/MM-LPS curves superimpose with each other

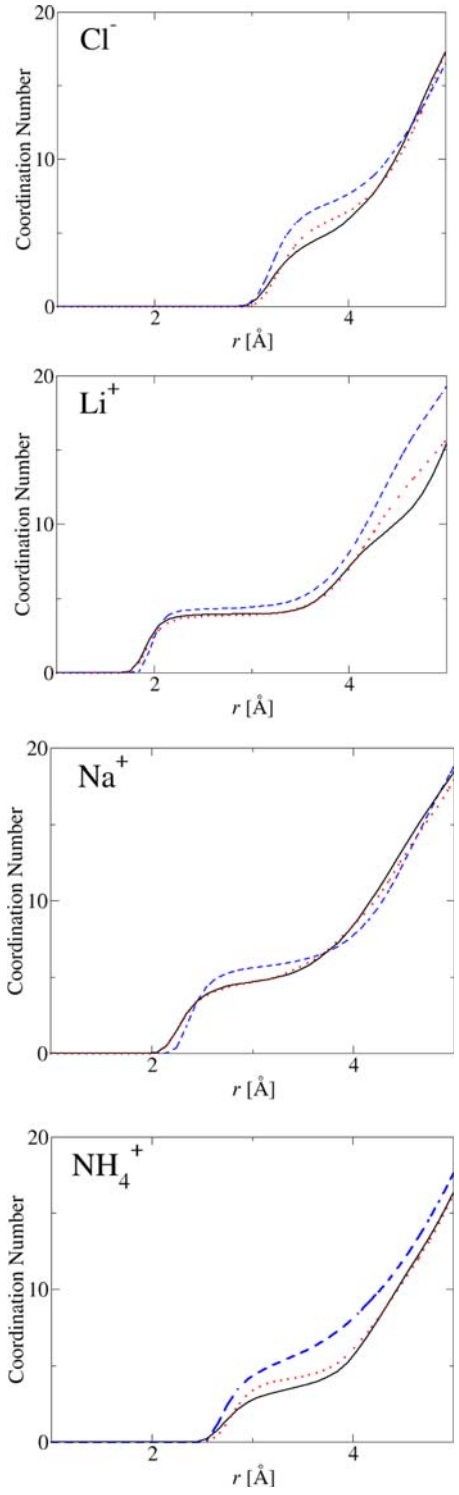

Figure 9. Integrated coordination numbers for the ions. The QM/MM-LPS results are shown by the solid curves, the FB-QM/MM results by the dotted curves, and the MM results by dashed curves.

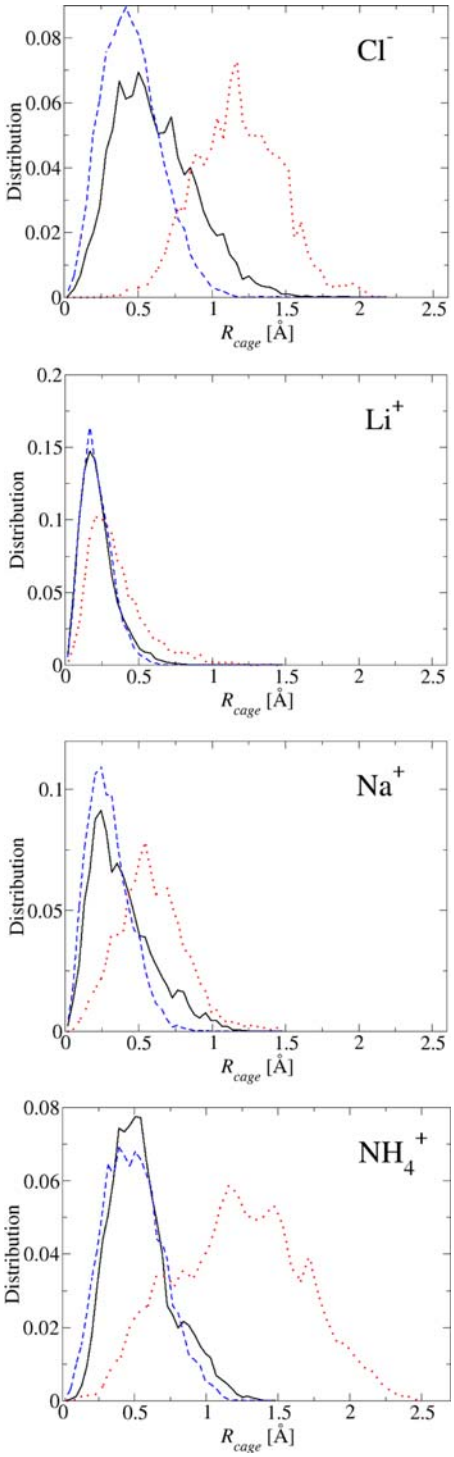

Figure 10. Distributions of the distance R_{cage} between a given ion and the center of mass of its first solvation shell. The QM/MM-LPS results are shown by the solid curves, the FB-QM/MM results by the dotted curves, and the MM results by dashed curves. [Color figure can be viewed in the online issue, which is available at wileyonlinelibrary.com.]

very well, while the MM simulations clearly overestimate the number of water molecules that are coordinating the ions by 1 to 2. In Figure 10, the distances R_{cage} between the ions and the centers of mass of their first-solvation shell water molecules are plotted. The plots provide information about the anisotropy of the solvation shells around the given ions.[90] Generally speaking, an ion with larger polarizability will lead to larger anisotropy. Compared with the QM/MM-LPS results, the FB-QM/MM simulations have increased the anisotropy. The increasing in anisotropy is especially notable for ions with larger sizes (Cl^- and NH_4^+). For example, R_{cage} by FB-QM/MM for Cl^- fluctuates between 0.3 and 2.0 Å, with a peak near 1.2 Å. As a comparison, the R_{cage} by QM/MM-LPS are between 0 and 1.5 Å, with the peak near 0.5 Å. The solvation shells in the MM simulations are even more symmetric, with R_{cage} between 0 and 1.1 Å and peak at 0.4 Å. For Li^+ and Na^+ of smaller size and smaller polarizability, the differences between the FB-QM/MM and QM/MM-LPS results are much less significant, as can be seen in Figure 10. Currently, it is not clear to us what causes the discrepancies between the FB-QM/MM and QM/MM-LPS results in this regard, although we suspect that the problem is due to the overestimations of the polarization and charge transfer for the ions in the FB-QM/MM calculations (see also Fig. 5).

Conclusions

In this work, the extension of the FB-QM/MM schemes for dynamics simulations has been implemented. To overcome the polarization catastrophe that may occur when the atoms are in close distances during simulations, additive penalty energies are introduced via correcting functions. The correcting functions are empirical amendments to the underestimated repulsive exchange forces while keeping the existing vdW parameters unchanged. Without those correction functions, we have found simulations crashed frequently. The applicability of the correcting functions is tested in simulations of four model systems for ion solvation. The amount of charge transfer between the PS and SS and the atomic charges of the PS are compared with QM/MM-LPS calculations. Also compared are the structural properties such as RDF, integrated coordination numbers, and symmetry of the solvation shells of the ions. While the agreements are not perfect, they are very encouraging, indicating that the FB-QM/MM can be of use in MD simulations.

The correcting functions that we have adopted in this study are a simple solution that can be implemented in a straightforward manner. It is certainly not a cure-all. Although the functional forms that we have used worked reasonably well in the present study, further efforts are needed in the future to develop more general and more accurate correcting algorithms that not only require less fitting parameters but also have better parameter transferability. The development of correcting algorithms may be combined with the reparameterization of the QEq model or other classical charge equalization models that are based on the concept of electronegativity. As noted earlier, the QEq parameters used in this work are taken directly from the literature and have not been specifically reoptimized for the FB-QM/MM schemes. The combination of the better correcting algorithms and more accurate QEq parameters should enhance the performance of FB-QM/MM in dynamics simulations.

Computational cost is an important factor in choosing a QM/MM scheme. In the current implementations of the FB schemes, the molar fraction of the oxidized and reduced states are determined variationally at each step of trajectory propagation. While doing so offers accuracy, it is not very efficient. It is strongly desirable to reduce the computational cost without scarifying much accuracy. For example, it should be possible to propagate the molar fractions as dynamical variables with extended Lagarangian formalism, which has been used quite often in many dynamics simulation algorithms, for example, in the Car–Parrinello dynamics[53] and in the dynamics simulations by the fluctuating charge force fields.[32] The use of extended Lagarangian formalism should improve the efficiency of the FB-QM/MM scheme, making it a competitive alternative in dynamics simulations where the QM/MM-LPS simulations are too expensive to apply.

Another highly desirable extension is to combine the FB scheme with the adaptive-QM/MM algorithms,[16,64,91–102] which treat the on-the-fly exchanges of atoms between the QM and MM subsystems. The combination of the FB and adaptive methods will lead to the open-boundary QM/MM,[16,18] which permits dynamical transfers of both partial charges and atoms at the same time between the QM and MM subsystem in MD simulations. The open-boundary QM/MM offers a seamless integration of QM and MM in dynamical and complex environments and will be very useful in the MD simulations of ion solvation and many other processes.

Keywords: chemical potential · electronegativity equalization · polarization · ion salvation · combined quantum mechanical /molecular mechanical

How to cite this article: S. Pezeshki, H. Lin, *J. Comput. Chem.* **2014**, *35*, 1778–1788. DOI: 10.1002/jcc.23685

Additional Supporting Information may be found in the online version of this article.

[1] A. Warshel, M. Levitt, *J. Mol. Biol.* **1976**, *103*, 227.
[2] U. C. Singh, P. A. Kollmann, *J. Comput. Chem.* **1986**, *7*, 718.
[3] M. J. Field, P. A. Bash, M. Karplus, *J. Comput. Chem.* **1990**, *11*, 700.
[4] J. Gao, *Rev. Comput. Chem.* **1996**, *7*, 119.
[5] R. A. Friesner, M. D. Beachy, *Curr. Opin. Struct. Biol.* **1998**, *8*, 257.
[6] J. Gao, M. A. Thompson, Eds. Combined Quantum Mechanical and Molecular Mechanical Methods: ACS Symp. Ser. 712; American Chemical Society: Washington, DC, **1998**.
[7] M. F. Ruiz-López, J. L. Rivail, In Encyclopedia of Computational Chemistry; P. von Ragué Schleyer, Ed.; Wiley: Chichester, **1998**; pp 437–448.
[8] G. Monard, K. M. Merz, Jr., *Acc. Chem. Res.* **1999**, *32*, 904.
[9] I. H. Hillier. *THEOCHEM* **1999**, *463*, 45.
[10] S. Hammes-Schiffer, *Acc. Chem. Res.* **2000**, *34*, 273.
[11] P. Sherwood, In Modern Methods and Algorithms of Quantum Chemistry; J. Grotendorst, Ed.; John von Neumann-Instituts: Jülich, **2000**; pp 285–305.
[12] J. Gao, D. G. Truhlar, *Annu. Rev. Phys. Chem.* **2002**, *53*, 467.
[13] K. Morokuma, *Philos. Trans. R. Soc. London, A* **2002**, *360*, 1149.
[14] H. Lin, D. G. Truhlar, *Theor. Chem. Acc.* **2007**, *117*, 185.
[15] H. M. Senn, W. Thiel, *Top. Curr. Chem.* **2007**, *268*, 173.
[16] S. Pezeshki, H. Lin, *Mol. Simul.* **2014**, DOI 10.1080/08927022.2014.911870, 1–22.
[17] Y. Zhang, H. Lin, *J. Chem. Theory Comput.* **2008**, *4*, 414.
[18] Y. Zhang, H. Lin, *Theor. Chem. Acc.* **2010**, *126*, 315
[19] W. J. Mortier, K. Van Genechten, J. Gasteiger, *J. Am. Chem. Soc.* **1985**, *107*, 829.
[20] W. J. Mortier, S. K. Ghosh, S. Shankar, *J. Am. Chem. Soc.* **1986**, *108*, 4315.
[21] K. T. No, J. A. Grant, H. A. Scheraga, *J. Phys. Chem.* **1990**, *94*, 4732.
[22] A. K. Rappé, W. A. Goddard, *J. Phys. Chem.* **1991**, *95*, 3358.
[23] J. Cioslowski, B. B. Stefanov, *J. Chem. Phys.* **1993**, *99*, 5151.
[24] S. W. Rick, S. J. Stuart, B. J. Berne, *J. Chem. Phys.* **1994**, *101*, 6141.
[25] F. De Proft, W. Langenaeker, P. Geerlings, *J. Mol. Struct.: THEOCHEM* **1995**, *339*, 45
[26] D. Bakowies, W. Thiel, *J. Comput. Chem.* **1996**, *17* 87.
[27] S. W. Rick, B. J. Berne, *J. Am. Chem. Soc.* **1996**, *118*, 672.
[28] D. M. York, W. Yang, *J. Chem. Phys.* **1996**, *104*, 159.
[29] Z.-Z. Yang, C.-S. Wang, *J. Phys. Chem. A* **1997**, *101*, 6315.
[30] P. Itskowitz, M. L. Berkowitz, *J. Phys. Chem. A* **1997**, *101*, 5687.
[31] P. Bultinck, W. Langenaeker, P. Lahorte, F. De Proft, P. Geerlings, M. Waroquier, J. P. Tollenaere, *J. Phys. Chem. A* **2002**, *106*, 7887.
[32] S. Patel, C. L. Brooks, III, *J. Comput. Chem.* **2004**, *25*, 1.
[33] S. Patel, A. D. Mackerell, Jr., C. L. Brooks, III, *J. Comput. Chem.* **2004**, *25*, 1504.
[34] P. M. Lopes, B. Roux, A. MacKerell, Jr., *Theor. Chem. Acc.* **2009**, *124*, 11.
[35] M. J. S. Dewar, J. A. Hashmall, C. G. Venier, *J. Am. Chem. Soc.* **1968**, *90*, 1953.
[36] M. J. S. Dewar, N. Trinajstic, *J. Chem. Soc. Chem. Commun.* **1970**, 646.
[37] V. Gogonea, K. M. Merz, Jr., *J. Chem. Phys.* **2000**, *112*, 3227.
[38] V. Gogonea, K. M. Merz, Jr., *J. Phys. Chem. B* **2000**, *104*, 2117.
[39] J. P. Perdew, R. G. Parr, M. Levy, J. L. Balduz, *Phys. Rev. Lett.* **1982**, *49*, 1691.
[40] Y. Zhang, W. Yang, *J. Chem. Phys.* **1998**, *109*, 2604.
[41] W. Yang, Y. Zhang, P. W. Ayers, *Phys. Rev. Lett.* **2000**, *84*, 5172.
[42] Y. Zhang, W. Yang, *Theor. Chem. Acc.* **2000**, *103*, 346.
[43] A. J. Cohen, P. Mori-Sanchez, W. Yang, *J. Chem. Phys.* **2008**, *129*, 121104/1-4.
[44] X. Zeng, H. Hu, X. Hu, A. J. Cohen, W. Yang, *J. Chem. Phys.* **2008**, *128*, 124510/1-10.
[45] A. J. Cohen, P. Mori-Sanchez, W. Yang, *J. Chem. Theory Comput.* **2009**, *5*, 786.
[46] D. H. Ess, E. R. Johnson, X. Hu, W. Yang, *J. Phys. Chem. A* **2011**, *115*, 76.
[47] S. N. Steinmann, W. Yang, *J. Chem. Phys.* **2013**, *139*, 074107/1-14.
[48] N. J. Mayhall, K. Raghavachari, *J. Chem. Theory Comput.* **2011**, *7*, 1336.
[49] P. Elliott, M. H. Cohen, A. Wasserman, K. Burke, *J. Chem. Theory Comput.* **2009**, *5*, 827.
[50] P. Elliott, K. Burke, M. H. Cohen, A. Wasserman, *Phys. Rev. A* **2010**, *82*, 024501/1-4.
[51] I. Tavernelli, R. Vuilleumier, M. Sprik, *Phys. Rev. Lett.* **2002**, *88*, 213002/1-4.
[52] Y. Zhang, H. Lin, D. G. Truhlar, *J. Chem. Theory Comput.* **2007**, *3*, 1378.
[53] R. Car, M. Parrinello, *Phys. Rev. Lett.* **1985**, *55*, 2471.
[54] P. Jungwirth, D. J. Tobias, *J. Phys. Chem. A* **2002**, *106*, 379.
[55] J. Sala, E. Guàrdia, M. Masia, *J. Chem. Phys.* **2010**, *133*(23),234101.
[56] E. Guàrdia, A. Calvo, M. Masia, *Theor. Chem. Acc.* **2012**, *131*, 1.
[57] A. P. Lyubartsev, K. Laasonen, A. Laaksonen, *J. Chem. Phys.* **2001**, *114*, 3120.
[58] Y. Zeng, C. Wang, X. Zhang, S. Ju, *Chem. Phys.* **2014**, *433*, 89.
[59] Y. Zeng, J. Hu, Y. Yuan, X. Zhang, S. Ju, *Chem. Phys. Lett.* **2012**, *538*, 60.
[60] W. Liu, R. H. Wood, D. J. Doren, *J. Chem. Phys.* **2003**, *118*, 2837.
[61] A. Tongraar, B. M. Rode, *Phys. Chem. Chem. Phys.* **2003**, *5*, 357.
[62] A. Ohrn, G. Karlstrom, *J. Phys. Chem. B* **2004**, *108*, 8452.
[63] A. Tongraar, B. M. Rode, *Chem. Phys. Lett.* **2005**, *403*, 314.
[64] K. Park, A. W. Gotz, R. C. Walker, F. Paesani, *J. Chem. Theory Comput.* **2012**, *8*, 2868.
[65] B. Lev, B. Roux, S. Y. Noskov, *J. Chem. Theory Comput.* **2013**, *9*, 4165.
[66] H. H. Loeffler, B. M. Rode, *J. Chem. Phys.* **2002**, *117*, 110.
[67] H. H. Loeffler, A. M. Mohammed, Y. Inada, S. Funahashi, *Chem. Phys. Lett.* **2003**, *379*, 452.
[68] A. Tongraar, K. R. Liedl, B. M. Rode, *J. Phys. Chem. A* **1998**, *102*, 10340.
[69] B. B. Lev, D. R. Salahub, S. Y. Noskov, *Interdiscip. Sci.* **2010**, *2*, 12.
[70] C. N. Rowley, B. Roux, *J. Chem. Theory Comput.* **2012**, *8*, 3526.
[71] P. Intharathep, A. Tongraar, K. Sagarik, *J. Comput. Chem.* **2005**, *26*, 1329.
[72] Y. Koyano, N. Takenaka, Y. Nakagawa, M. Nagaoka, *Bull. Chem. Soc. Jpn.* **2010**, *83*, 486.

[73] B. M. Rode, C. F. Schwenk, T. S. Hofer, B. R. Randolf, *Coord. Chem. Rev.* **2005**, *249*, 2993.
[74] A. A. Hassanali, J. Cuny, V. Verdolino, M. Parrinello, *Philos. Trans. R. Soc. A* **2014**, 372.
[75] P. Ren, J. Chun, D. G. Thomas, M. J. Schnieders, M. Marucho, J. Zhang, N. A. Baker, *Q. Rev. Biophys.* **2012**, *45*, 427.
[76] C. C. J. Roothaan, *Rev. Mod. Phys.* **1951**, *23*, 69.
[77] R. Ditchfield, W. J. Hehre, J. A. Pople, *J. Chem. Phys.* **1971**, *54*, 724.
[78] W. J. Hehre, R. Ditchfield, J. A. Pople, *J. Chem. Phys.* **1972**, *56*, 2257.
[79] M. M. Francl, W. J. Pietro, W. J. Hehre, J. S. Binkley, D. J. DeFrees, J. A. Pople, M. S. Gordon, *J. Chem. Phys.* **1982**, *77*, 3654.
[80] M. J. Frisch, J. A. Pople, J. S. Binkley, *J. Chem. Phys.* **1984**, *80*, 3265.
[81] W. L. Jorgensen, D. S. Maxwell, J. Tirado-Rives, *J. Am. Chem. Soc.* **1996**, *118*, 11225.
[82] R. C. Rizzo, W. L. Jorgensen, *J. Am. Chem. Soc.* **1999**, *121*, 4827.
[83] G. A. Kaminski, R. A. Friesner, J. Tirado-Rives, W. L. Jorgensen, *J. Phys. Chem. B* **2001**, *105*, 6474.
[84] K. Kahn, T. C. Bruice, *J. Comput. Chem.* **2002**, *23*, 977.
[85] H. J. C. Berendsen, J. P. M. Postma, W. F. v. Gunsteren, J. Hermans, In Intermolecular Forces; B. Pullman, Ed.; D. Reidel Publishing Company: Dordrecht, **1981**; pp 331–342.
[86] H. Lin, Y. Zhang, S. Pezeshki, D. G. Truhlar, QMMM 2.0.0.CO, University of Minnesota: Minneapolis, **2012**.
[87] J. W. Ponder, TINKER 5.1, Washington University: St. Louis, MO, **2010**.
[88] M. J. Frisch, G. W. Trucks, H. B. Schlegel, G. E. Scuseria, M. A. Robb, J. R. Cheeseman, J. Montgomery, J. A., T. Vreven, K. N. Kudin, J. C. Burant, J. M. Millam, S. S. Iyengar, J. Tomasi, V. Barone, B. Mennucci, M. Cossi, G. Scalmani, N. Rega, G. A. Petersson, H. Nakatsuji, M. Hada, M. Ehara, K. Toyota, R. Fukuda, J. Hasegawa, M. Ishida, T. Nakajima, Y. Honda, O. Kitao, H. Nakai, M. Klene, X. Li, J. E. Knox, H. P. Hratchian, J. B. Cross, C. Adamo, J. Jaramillo, R. Gomperts, R. E. Stratmann, O. Yazyev, A. J. Austin, R. Cammi, C. Pomelli, J. W. Ochterski, P. Y. Ayala, K. Morokuma, G. A. Voth, P. Salvador, J. J. Dannenberg, V. G. Zakrzewski, S. Dapprich, A. D. Daniels, M. C. Strain, O. Farkas, D. K. Malick, A. D. Rabuck, K. Raghavachari, J. B. Foresman, J. V. Ortiz, Q. Cui, A. G. Baboul, S. Clifford, J. Cioslowski, B. B. Stefanov, G. Liu, A. Liashenko, P. Piskorz, I. Komaromi, R. L. Martin, D. J. Fox, T. Keith, M. A. Al-Laham, C. Y. Peng, A. Nanayakkara, M. Challacombe, P. M. W. Gill, B. Johnson, W. Chen, M. W. Wong, C. Gonzalez, J. A. Pople, *GAUSSIAN03,* Gaussian, Inc.: Pittsburgh, PA, **2003**.
[89] H. J. C. Berendsen, J. P. M. Postma, W. F. v. Gunsteren, A. DiNola, J. R. Haak, *J. Chem. Phys.* **1984**, *81*, 3684.
[90] Z. Zhao, D. M. Rogers, T. L. Beck, *J. Chem. Phys.* **2010**, *132*, 014502/1-10.
[91] T. Kerdcharoen, K. R. Liedl, B. M. Rode, *Chem. Phys.* **1996**, *211*, 313.
[92] T. Kerdcharoen, K. Morokuma, *Chem. Phys. Lett.* **2002**, *355*, 257.
[93] T. Kerdcharoen, K. Morokuma, *J. Chem. Phys.* **2003**, *118*, 8856.
[94] A. Heyden, H. Lin, D. G. Truhlar, *J. Phys. Chem. B* **2007**, *111*, 2231.
[95] R. E. Bulo, B. Ensing, J. Sikkema, L. Visscher, *J. Chem. Theory Comput.* **2009**, *5*, 2212.
[96] M. G. Guthrie, A. D. Daigle, M. R. Salazar, *J. Chem. Theory Comput.* **2009**, *6*, 18.
[97] S. O. Nielsen, R. E. Bulo, P. B. Moore, B. Ensing, *Phys. Chem. Chem. Phys.* **2010**, *12*, 12401.
[98] A. B. Poma, L. Delle Site, *Phys. Rev. Lett.* **2010**, *104*, 250201/1-4.
[99] S. Pezeshki, H. Lin, *J. Chem. Theory Comput.* **2011**, *7*, 3625.
[100] N. Bernstein, C. Varnai, I. Solt, S. A. Winfield, M. C. Payne, I. Simon, M. Fuxreiter, G. Csanyi, *Phys. Chem. Chem. Phys.* **2012**, *14*, 646.
[101] N. Takenaka, Y. Kitamura, Y. Koyano, M. Nagaoka, *Chem. Phys. Lett.* **2012**, *524*, 56.
[102] C. Várnai, N. Bernstein, L. Mones, G. Csányi, *J. Phys. Chem. B* **2013**, *117*, 12202.

Received: 16 April 2014
Revised: 19 June 2014
Accepted: 30 June 2014
Published online on 23 July 2014